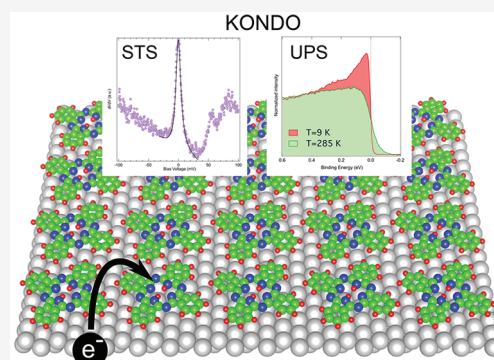


## Adsorption-Induced Kondo Effect in Metal-Free Phthalocyanine on Ag(111)

J. Granet, M. Sicot,\* I. C. Gerber, G. Kremer, T. Pierron, B. Kierren, L. Moreau, Y. Fagot-Revurat, S. Lamare, F. Chérioux, and D. Malterre

**ABSTRACT:** We report on the formation of a two-dimensional supramolecular Kondo lattice made of organic molecules comprising only C, N, and H atoms, namely metal-free phthalocyanines 2HPc ( $C_{32}H_{18}N_8$ ), adsorbed on a Ag(111) surface. Low-temperature scanning tunneling microscopy/spectroscopy (LT-STM/STS), ultraviolet photoemission spectroscopy (UPS), and density functional theory (DFT) are used to investigate the electronic structure of the system for low molecular density and commensurate self-assemblies. Abrikosov–Suhl resonances that are characteristic of the arising of a Kondo effect are observed by using both STS and UPS at low temperature. Whereas freestanding 2HPc is a no-spin-bearing molecule, it acquires an unpaired electron in its  $\pi$ -conjugated lowest unoccupied molecular orbital (LUMO) upon adsorption on Ag. As a result, the Kondo effect can be interpreted as originating from the interaction between this unpaired  $\pi$ -spin and the Ag Fermi sea. Extra side resonances are observed in STS spectra that are a manifestation of the coupling between the  $\pi$  electron and molecular vibrational excitations, qualifying the effect as the molecular vibrational Kondo effect. The variation of the Kondo temperature  $T_K$  of single molecules and upon two-dimensional self-assembly is discussed. This study brings new insights into the Kondo-related physics in correlation with molecular spins and low dimensionality. Moreover, it may open new routes to the synthesis of organic molecular spintronic devices.



### INTRODUCTION

Molecular magnetism has attracted increasing attention since molecular based magnetic materials can have many technological applications in areas such as quantum computation,<sup>1,2</sup> high-density data storage, and spintronics.<sup>3–7</sup> Very early in the development of the field, metallophthalocyanines (MPcs) have proven to be a privileged class of molecules to study magnetism at the nanometer scale.<sup>8–11</sup> Indeed, many MPcs possess unpaired electrons in the gas phase and thus have nonzero magnetic moments. Besides, bis-phthalocyanines sandwiching rare-earth ions have been shown to behave as single molecular magnets.<sup>12,13</sup> Their applicative potential has already been demonstrated, for example, by fabricating functional supramolecular spin valves.<sup>14</sup>

The attractiveness of these molecules also lies in their easy synthesis, low cost, and industrial availability. Particularly, they can be evaporated under ultrahigh vacuum (UHV) allowing the synthesis of thin films.<sup>15</sup> In addition, the planar geometry of their  $\pi$ -conjugated ligand that can lie parallel to the surface on which they are adsorbed is an asset: the flatness of MPcs allows direct hybridization with the orbitals of the underlying substrate, leading to the modification of surface properties and new exotic phenomena when in contact with various substrates such as ferromagnetic (FM) materials,<sup>4</sup> topological insulators,

superconductors, or 2D materials.<sup>16–18</sup> For instance, in the case of the MPc/FM molecular spinterfaces, it has been shown that the addition of MPc increases or inverts the FM spin polarization, which is a key property regarding the performance of spin devices.<sup>19–22</sup> In the case of CoPc/Bi<sub>2</sub>Se<sub>3</sub>, Caputo et al. have evidenced by angular-resolved photoelectron spectroscopy (ARPES) the modification of the topological surface states and the energy shift of the Dirac cone due to charge transfer from the molecule to the surface.<sup>23</sup> When in contact with superconductors, magnetic nano-objects can be envisaged as qubits for quantum computing devices. In such cases, the governing factor is the strength of spin–superconductor interactions. MPc/Pb(111) interfaces have been shown to be ideal platforms to tune locally this magnetic interaction strength by adsorbing the molecules on different sites or by continuously varying it using the interaction with an STM tip.<sup>24,25</sup> Finally, optical measurements of MPc/MoS<sub>2</sub> hetero-

junctions evidenced charge transfer that is sensitive to the transition metal core. This property allows for tunable optical absorption, making those systems interesting for optoelectronic applications.<sup>16</sup>

Moreover, this flat-lying molecular adsorption configuration offers an open area to the vacuum side. This gives the opportunity to manipulate the spin state by using on-top adsorption of alkali atoms or molecules to induce electron doping. Such studies have led to the emerging research field of surface magnetochemistry.<sup>26,27</sup>

In many cases, interfacial properties result from the hybridization of the highly directional  $d_{z^2}$  orbital of the core metal atom with those of the substrate. Yet, for other MPC/inorganic interfaces, coupling can arise from hybridization with the  $\pi$  ( $p_z$ ) orbital of the Pc ligand as well. The filling of the  $\pi$  orbital by charge transfer modifies the spin state of the molecule in comparison with the free one. As an example, it was shown that the no-spin-bearing NiPc molecule acquires a 1/2 spin of  $\pi$ -origin due to charge transfer upon adsorption on a Ag(100) single-crystalline surface.<sup>28,29</sup> This has been demonstrated by revealing the spectral signature, which is typical of a 1/2-spin object in interaction with an electron bath, namely an Abrikosov–Suhl resonance of the differential conductance in the vicinity of the Fermi level  $E_F$  by using LT-STM/STS resulting from the Kondo effect.<sup>30–35</sup> On the same Ag(100) surface, CuPc, which possesses a 1/2-spin state in its ground state, acquires an extra  $\pi$ -electron. In this last case, the molecule behaves as a two-spin system in contact with conduction electrons, leading to an interesting many-body phenomenon: a triplet–singlet Kondo effect.<sup>28</sup> Alternatively, STM and UPS measurements recorded on the CoPc/Ag(111) interface have unravelled another more complex donation/back-donation scenario: electron injection occurs from the Ag substrate to the Co 3d orbitals that is accompanied with a back-donation of electrons from the  $\pi$  orbitals to the substrate.<sup>36</sup>

Recently, it was shown by UPS that the metal-free phthalocyanine 2HPc, which is a no-spin-bearing molecule in the gas phase, can also become charged upon adsorption on Ag(111).<sup>37–39</sup> We can therefore wonder whether this system could also exhibit a Kondo effect as in the case of NiPc or CuPc on Ag(100). The implication of such a result would be that a purely organic phthalocyanine adsorbed on a silver surface could give rise to interesting magnetic properties without the involvement of 3d transition-metal or 4f rare-earth central ions as in previous studies. Indeed, only very few examples of pure organic systems presenting the Kondo effect have been reported so far.<sup>40–45</sup>

Despite the increasing attention devoted to the above-mentioned hybrid MPC/inorganic interfaces, however, the spin-polarized electronic properties of the 2HPc/Ag(111) interface had been overlooked.<sup>37–39,46</sup> Yet, this particular system could provide a means of investigating many-body phenomena such as the Kondo effect in many aspects, e.g., its intensity, spatial extension,<sup>47</sup> and quantum criticality<sup>44</sup> when a 1/2 spin in a  $\pi$  orbital is involved rather than a 3d or 4f orbital. It would therefore broaden our knowledge on magnetism as well as on many-body physics at the nanometer scale and at low dimensionality.<sup>40–43,47–62</sup> Moreover, as illustrated above, a full description of the hybrid interfaces must necessarily consider both interfacial sides. On the metal side, sizable modifications can also be expected as already observed with other  $\pi$ -conjugated molecules at the interface with copper or

silver surfaces.<sup>39,63–67</sup> In the case of 2HPc/Ag(111), it has been shown that upon molecular adsorption an interfacial state forms originating from the well-known bare metal Shockley state.<sup>39,68,69</sup> Those hybrid interfacial states (HIS) are of particular importance for the understanding of contact in organic semiconductor devices and their origin are not yet fully understood.<sup>63,67</sup> Therefore, such a study might also unravel insights into the Ag hybrid interface state.

In this framework, we have investigated by LT-STM/STS, UPS, and DFT the electronic structure of adsorbed 2HPc on Ag(111) for single molecules as well as for two-dimensional self-assembled molecular networks. We demonstrate the emergence of a Kondo effect regardless of the coverage in the submonolayer regime. We think that this kind of hybrid interface with molecules comprising only C, H, and N atoms may thus be envisaged to design metamaterials composed of abundant and environmental-friendly compounds.

## ■ METHODS

The experiments were performed in two ultrahigh-vacuum systems with a base pressure of  $1 \times 10^{-10}$  mbar. One was equipped with a low-temperature Omicron STM operating at 5 K. The other one was equipped with a Scienta Omicron DA30-L hemispherical analyzer and a monochromatized He<sub>I</sub> ( $h\nu = 21.2$  eV) UV source for ARPES. As the beam damage of the molecular layers was observed on a time scale of about 20 min, the duration of the measurements and sample position were adjusted accordingly. Because of angular distribution of the photoemission intensity, ultraviolet photoemission spectra were recorded at an emission angle of  $45^\circ$ .<sup>54,70,71</sup> Note that in this geometry the Shockley surface state of Ag(111) lying in the L-gap around the  $\Gamma$  point of the surface Brillouin zone is not detected.<sup>69</sup> All spectra were normalized to the count rate at the binding energy of 0.4 eV. LEED was available on both UHV setups to characterize structural properties at a sample temperature of 80 K. The Ag(111) single crystal was cleaned by repeated cycles of Ar<sup>+</sup> sputtering at an energy of 1 keV followed by an annealing to 800 K. 2HPc molecules were purchased from Aldrich and purified by column chromatography (silica gel, dichloromethane) prior to use. They were evaporated from a Knudsen cell at 565 K onto the sample held at room temperature. The STM images were recorded at a tunneling current  $I_t$  and a bias voltage  $V_b$  where the sign corresponds to the voltage applied to the sample. STS was acquired with a PtIr scissors-cut tip and a lock-in detection in open feedback loop conditions at a frequency of 1100 Hz and a peak-to-peak bias voltage modulation for high-resolution STS of 5 mV.

The electronic structures were obtained from DFT calculations with the VASP package<sup>72–75</sup> which uses the projector-augmented wave scheme<sup>76,77</sup> to treat core electrons. The Perdew–Burke–Ernzerhof (PBE) functional<sup>78</sup> was used as an approximation of the exchange–correlation electronic term, but the PBE-D3 scheme<sup>79,80</sup> was used first to optimize the geometry since Huang et al. have addressed the importance of van der Waals corrections when dealing with Pc–metallic surface interactions.<sup>81</sup> The kinetic energy cutoff was set to 400 eV, with a Gaussian smearing of 0.05 eV and using a  $2 \times 2 \times 1$   $k$ -points grid to optimize the structures with a convergence force criterion of 0.01 eV/Å for all allowed atoms to relax. For density of states (DOS) determinations, a  $3 \times 3 \times 1$   $k$ -points grid was used in conjunction with the tetrahedron method with the Blöchl corrections scheme.<sup>82</sup> We have confirmed that a 12-

layer slab with a vacuum height of more than 20 Å was necessary to describe accurately the intrinsic Shockley surface state of the Ag (111) surface;<sup>83</sup> see Figure S3 for a band structure representation. As expected, two surface states are provided by the slab approach, and the average energy of the two surface states (−86 meV) is relatively close to the experimental energy value (−63 meV).<sup>69</sup> To mimic the individual molecule case, as well as to describe the C-phase (see definition below), a (7 × 7) and commensurate ([5 0; 3 6]) cell was used.

## RESULTS AND DISCUSSION

**Structural Properties.** The growth of 2HPc on Ag(111) in the submonolayer regime has been studied in previous works. Three distinct phases form as a function of the coverage.<sup>38</sup> For self-assemblies, the unit cells have been determined.<sup>38</sup> Yet, the adsorption geometry and especially the azimuthal orientation of the molecules have only succinctly been addressed and remain elusive, particularly in self-assemblies. Nevertheless, this information is of paramount importance to elucidate the electronic properties of the metal–organic interface. Thanks to STM images with intramolecular resolution, we were able to tackle this key point as will be explained below.

According to Kröger et al., at low molecular densities, 2HPc form disordered gaslike phases, referred to as G-phases where the intermolecular distance changes with coverage due to substrate-mediated intermolecular repulsive interaction.<sup>38</sup> Upon increasing coverages to 0.5–0.89 monolayers at low temperature, they form a commensurate phase with the substrate referred to as the C-phase, characterized by a nearly square unit cell in which the epitaxy matrix is [5 0; 3 6].<sup>38</sup> Our LEED patterns displayed in Figures 1a and 2a exhibiting a diffuse ring around the [00] specular beam and sharp spots, respectively, are in line with those previous results. Sperl et al. showed that 2HPc adsorbs flat onto the Ag(111) substrate; i.e., the Pc ligand plane adsorbs parallel to the surface plane.<sup>46</sup> The line formed by the two pyrrolic hydrogen atoms inside the porphyrazine core, which will be referred to as “the 2H-axis” hereafter, was shown to be azimuthally oriented perpendicular to  $\langle 01\bar{1} \rangle$  crystallographic directions of the substrate. This was later confirmed by Kügel et al.<sup>84</sup> In the C-phase, Bai et al. measured by STM an azimuthal angle between one vector of the unit cell and the molecular axis of about  $60 \pm 3^\circ$  without specifying the orientation of the 2H-axis.<sup>85</sup> In the present work, we determine the orientation of single molecules by comparing their STM appearance in Figure 1b with the HOMO of the singly charged 2HPc anion calculated in ref 86 for which the split lobes are perpendicular to the 2H-axis. The specific choice of comparison with the anion is justified by the fact that the molecule gets negatively charged when adsorbed as we will discuss below. The direction of the 2H-axis of the molecules is highlighted by blue lines in Figure 1b. Our STM images reveal that 2HPc adsorbs with the 2H-axis not only perpendicular to  $\langle 01\bar{1} \rangle$  directions (i.e., along  $\langle 2\bar{1}\bar{1} \rangle$  directions) as observed in the literature<sup>46,84</sup> but also parallel (within an angle error of  $\pm 2^\circ$ ). Molecules marked as C and C' in Figure 1b are representative of the two configurations. Likewise in Figure 1c, molecules A and B adsorb in the same configuration as molecule C. In their recent work, Kügel and co-workers demonstrate that the only way to obtain a 2H-axis along one of the  $\langle 01\bar{1} \rangle$  directions is to start with a molecule in which the

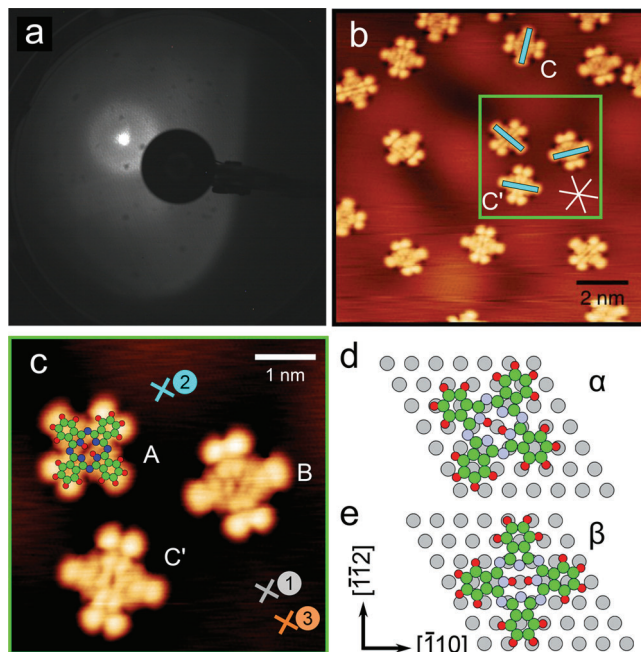


**Figure 1.** Structure of 2HPc/Ag(111) in G-phase. (a) LEED pattern recorded at an electron energy of 15 eV. (b, c) High-resolution STM topographic images of 2HPc molecules on Ag(111). Tunneling bias conditions:  $V_b = 1$  mV,  $I_t = 200$  pA. The close-packed  $\langle 01\bar{1} \rangle$  directions of the Ag(111) are indicated by white lines in (b). The numbered crosses in (c) indicate the location where the STS spectra displayed in Figures 3a and 5a were recorded. Cyan lines in (b) indicate the direction of the 2H-axis (see text) of the molecules. (d, e) Top views of the DFT calculated relaxed most stable adsorption geometries.

2H-axis is perpendicular to one  $\langle 01\bar{1} \rangle$  direction and induce tautomerization by applying a bias voltage pulse  $U$  such that  $|U| > 0.45$  V when the tip is located above the molecule. It is claimed that the absence of the 2H-axis along  $\langle 01\bar{1} \rangle$  directions can be explained by a high difference in energy with the configuration where the 2H-axis lies perpendicular to  $\langle 01\bar{1} \rangle$ .

On the contrary, in our work, we find two adsorption orientations that can simply be explained by molecules that could rotate in the ligand plane. Figure 1d,e displays the two simulated most stable adsorption configurations  $\alpha$  and  $\beta$  corresponding to 2H perpendicular and parallel to  $\langle 01\bar{1} \rangle$  directions, respectively, in good agreement with our observations. The difference of adsorption energy between these two geometries of minimum energy is only of about 0.2 eV. Molecules A, B, and C would therefore correspond to the  $\alpha$ -case (Figure 1d), whereas molecule C' would correspond to the  $\beta$ -case (Figure 1e). From these models, one can see that the transition from one geometry to the other can occur simply via a rotation of the molecule by  $30^\circ$ . In our work, we found compelling evidence that such rotation can happen. In Figure S4, two time sequences issued from pairs of STM images recorded successively show molecules that rotate without external stimuli other than the scanning tip governed by the tunneling parameters  $V_b$  and  $I_t$  with  $V_b$  much smaller than the bias voltage threshold necessary to induce tautomerization. For the particular coverage shown in Figure 1b, the ratio of parallel to perpendicular configurations is 1/3, leading to the conclusion that the perpendicular geometry is the most stable one.

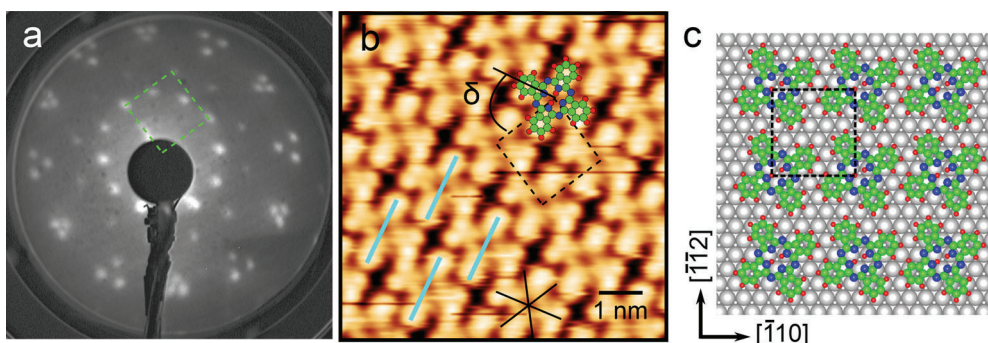


**Figure 2.** Structure of 2HPc/Ag(111) in the C-phase. (a) LEED pattern recorded at an electron energy of 14 eV. (b) Corresponding STM topographic image. Tunneling bias conditions:  $V_b = -1.8$  V,  $I_t = 200$  pA. The close-packed  $\langle 01\bar{1} \rangle$  directions of the Ag(111) are indicated by a black star. Cyan lines indicate the direction of the 2H-axis of the molecules (see text). (c) Top view of the simulated relaxed adsorption geometry. Rectangles in dashed line represent the unit cells in (a) reciprocal and (b, c) direct space.

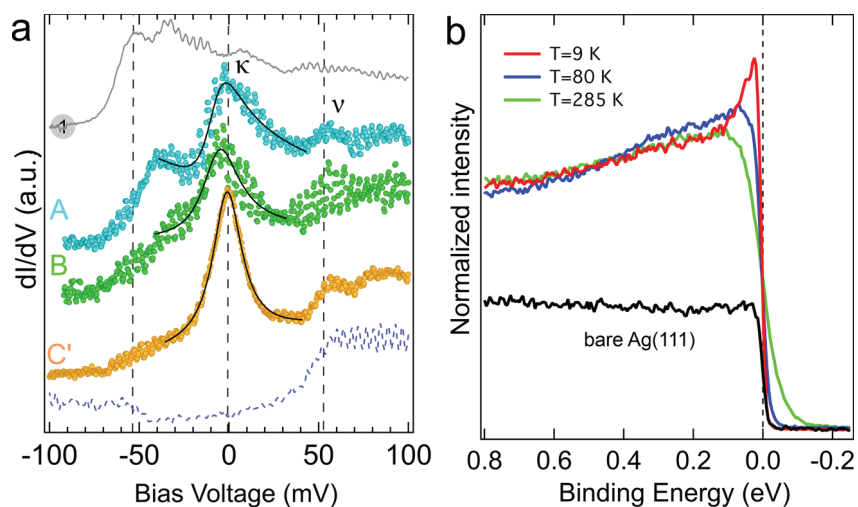


**Figure 3.** Electronic properties of 2HPc/Ag(111) in the G-phase. (a) Dotted lines are  $dI/dV$  spectra recorded with the tip on top of molecules labeled A, B, and C' in Figure 1c. The set point is  $V_b = 1$  mV,  $I_t = 200$  pA. The dashed blue line is a  $dI/dV$  spectrum recorded on a fourth molecule (not in Figure 1c). Set point:  $V_b = 25$  mV,  $I_t = 200$  pA. The full gray line was recorded further away from the molecules on a bare Ag surface at the position indicated by the gray cross in Figure 1c. The Fano fits represented by the black lines yields (A)  $q = 1.73$ ,  $\epsilon_K = -7.99$  meV, and  $\Gamma = 11.78$ , (B)  $q = 7.22$ ,  $\epsilon_K = -6.25$  meV, and  $\Gamma = 12.39$ , and (C')  $q = 54$ ,  $\epsilon_K = -1.16$  meV, and  $\Gamma = 9.8$ . A vertical shift was added for clarity. (b) UPS spectra recorded at  $T = 9, 80,$  and  $285$  K and on bare Ag(111) substrate at  $T = 9$  K (black line) and at an emission angle of  $45^\circ$ .

In the STM image of the C-phase displayed in Figure 2b, each molecule exhibits a pair of split lobes. Assuming that they are perpendicular to the 2H-axis as in the case of molecules in the G-phase, the azimuthal angle  $\delta$  with respect to the close-packed directions of Ag(111) as sketched in Figure 2b can be determined. The measured value of  $\delta$  is  $65 \pm 3^\circ$  similar within the angle error to the azimuthal orientation of the experimentally most stable adsorption configuration  $\alpha$ . The structural model of the molecules self-organized as a C-phase obtained by DFT calculations is shown in Figure 2c. The angle  $\delta = 62^\circ$  is in excellent agreement with the experimental value, validating this model to further extract the projected density of states (PDOS). The extra insight we get from this STM analysis is that molecules in the less stable configuration such as molecule C' in Figure 1b undergo an azimuthal rotation of about  $30^\circ$  upon self-assembling. Therefore, one expects the ratio between the two configurations to increase when increasing the coverage in favor of  $\alpha$  configuration. However, this analysis is out of the range of this paper.

**Kondo Effect in Single Molecules.** In previous works, it was demonstrated from UPS and two-photon photoemission (TPPE) measurements that charge transfer occurs from the

Ag(111) substrate to the Pc ligand of 2HPc.<sup>38,39</sup> In the C-phase, this was evidenced by the occupancy of the LUMO orbital upon adsorption, resulting in a state located at an energy of  $-0.15$  eV, and which has been called former-LUMO (F-LUMO) in reference to the LUMO state of the free molecule. In addition, an unoccupied HIS develops from the former Shockley-type electronic state of the bare Ag(111) surface. It originates from the steepening of the surface potential upon molecular adsorption. This nearly free electron state has been characterized by a band onset located at an energy of  $+0.23 \pm 0.03$  eV above  $E_F$ .<sup>39</sup> Knowing the above-mentioned results, one can reasonably raise the following question: would self-assembled 2HPc behave like 1/2-spin in contact with a free electron bath, possibly giving rise to Kondo effect? Would this effect persists for single molecules? To elucidate the arising of a Kondo effect for a single molecule as well as for a self-assembly, we performed STS and UPS on G- and C-phases.

First, we address the Kondo effect in single molecules using STS and UPS. STS spectra in the energy range around  $E_F$  are reported in Figure 3a. They were recorded with the STM tip located above molecules A, B, and C' displayed in Figure 1c.

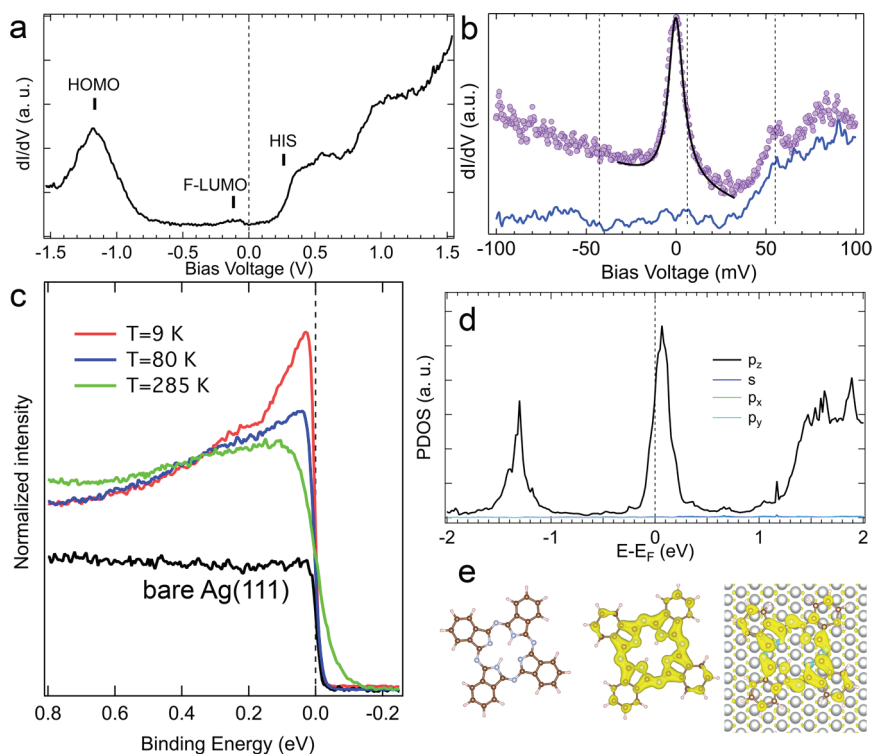


**Figure 4.** Electronic properties of 2HPc/Ag(111) in the C-phase. (a, b)  $dI/dV$  spectra recorded over the center of one molecule in the self-assembly. Set point are (a)  $V_b = -1$  V,  $I_t = 100$  pA and (b)  $V_b = 1$  mV,  $I_t = 200$  pA for top curve and  $V_b = 50$  mV,  $I_t = 200$  pA for bottom curve. A vertical shift was added for clarity. The Fano fit represented by the black line superimposed to the top curve in (b) yields  $q = 21$ ,  $\epsilon_K = -0.35$  meV, and  $\Gamma = 5.0$ . (c) UPS spectra recorded at  $T = 9$ , 80, and 285 K and on bare Ag(111) substrate at  $T = 9$  K at an emission angle of  $45^\circ$ . (d) Computed density of states projected (PDOS) onto atomic orbitals of 2HPc on Ag(111). (e) From left to right: spin density distribution of neutral, anionic 2HPc species in the gas phase, and adsorbed on Ag(111). The sign of the spin is indicated in yellow/cyan. The isovalue for the electronic spin density is roughly  $10^{-7}$  e/ $\text{\AA}^3$  in both cases.

All tunneling spectra show two main characteristics: (i) a sharp electronic resonance in the close vicinity of  $E_F$ , labeled  $\kappa$  in Figure 3a, and (ii) a conductance peak located at about +52 meV, labeled  $\nu$ . As no molecular nor substrate's state is expected in a range of  $\pm 10$  meV around  $E_F$ , we can, as a first guess, reasonably attribute the resonance at  $E_F$  to the Kondo effect. Yet, as other phenomena could lead to the formation of a peak in the differential conductance spectrum next to  $E_F$ , a magnetic field or temperature dependency of the full width at half-maximum (FWHM) of the resonance should be recorded and compared to laws governing the effect to unambiguously attribute its origin to the Kondo effect.<sup>87,88</sup> Alternatively, UPS can be used since a typical spectrum of a Kondo system exhibits a sharp resonance at  $E_F$  at temperatures below the Kondo temperature,  $T_K$ .<sup>87,89,90</sup> Upon increasing temperature, this peak is expected to broaden and decrease in intensity.<sup>91–93</sup> Such a relationship with temperature is what is experimentally observed as displayed in Figure 3b, showing UPS spectra recorded at temperatures of 9, 80, and 285 K. At  $T = 9$  K, a narrow and intense peak is observed at  $E_F$ . At  $T = 80$  K, the peak is broader and its intensity is strongly reduced to finally almost vanish at  $T = 285$  K.

The resonance observed in UPS spectra cannot be assigned to any state of the substrate since the UPS spectrum recorded under the same experimental conditions on the bare Ag(111) surface is flat next to  $E_F$ , as shown as a black line in Figure 3b. Thanks to the concomitance of a resonance at  $E_F$  in the STS spectrum and the temperature behavior of the photoemission

feature at  $E_F$ , one can now unambiguously attribute it to a Kondo resonance.

The next feature of the STS spectra to be discussed is the peak  $\nu$  at  $E_\nu = 52 \pm 5$  meV. This side feature appears as a resonance, and its intensity with respect to the zero-bias one depends on the tip location. Upon certain tip conditions (see the Supporting Information for further details), the Kondo resonance is not observed. In those cases, the  $dI/dV$  spectrum has an upside-down hat shape as depicted in Figure 3a. The two step edges are located at about  $\pm E_\nu$  which is the standard line shape observed when inelastic processes corresponding to vibrational excitation energies of  $E_\nu$  get activated. However, the side feature appears more as a resonance than as a step. According to refs 94–98, it can be understood as originating from the splitting of the zero-bias resonance resulting from the electron–vibron coupling. Other Kondo organic/inorganic systems exhibit as well such peaks of vibronic nature.<sup>28,29,40,99,100</sup> In particular, conductance spectra recorded over CuPc and NiPc on Ag(100) exhibit such fingerprints at comparable excitation energies<sup>28,29</sup> and might correspond to the activation of torsion modes.<sup>101</sup>

According to refs 32 and 33,  $T_K$  can be roughly determined by fitting the Kondo resonance with a Fano function line shape expressed as disregarding the instrumental broadening:<sup>102,103</sup>

$$\frac{(q + \epsilon)^2}{1 + \epsilon^2}; \quad \epsilon = \frac{eV - \epsilon_k}{\Gamma} \quad (1)$$

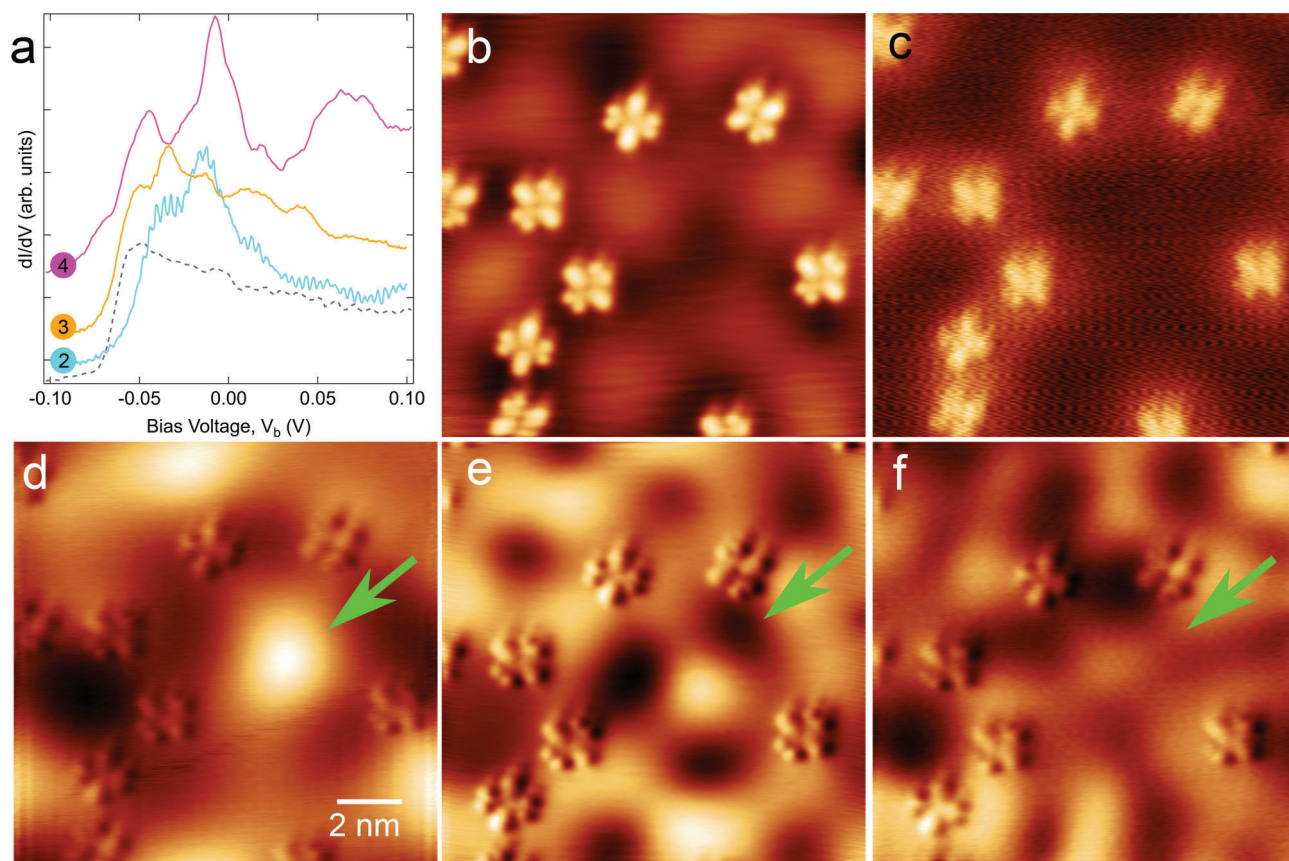


**Figure 5.** Electronic properties of Ag in G-phase. (a)  $dI/dV$  spectra recorded on Ag(111) between molecules in solid lines and on a pristine Ag(111) surface in the dashed line. Numerical labels 2–4 correspond to the position of the tip marked by a matching colored cross in Figure 1c and Figure S4b. Tunneling bias conditions:  $V_b = -1.8$  V,  $I_t = 200$  pA. (b) STM topographic image. Tunneling bias conditions:  $V_b = -40$  mV,  $I_t = 200$  pA. (c–f)  $dI/dV$  maps recorded at  $-100$ ,  $-40$ ,  $+10$ , and  $+30$  mV, respectively. Tunneling current  $I_t = 200$  pA.

where  $\Gamma$  is 1/2 FWHM such that  $\Gamma = k_B T_K$ ,  $q$  is the Fano asymmetry parameter, and  $\epsilon_k$  is the energy shift of the resonance from  $T_K$ .

As an example, the fitting results of the  $dI/dV$  spectra recorded at the center of molecules A, B, and C' are reported in Figure 3a as black lines. Another set of four measurements is shown in Figure S1. The mean fitted  $T_K$  is  $T_K = 130$  K with a standard deviation of 20 K, and  $q$  ranges from 0.3 to more than 50. The high  $q$  values indicate that the tunneling process occurs preferentially through the molecular orbital than to the conduction-electron continuum. Strong line shape and FWHM variations are observed between the molecules. The possible influence of the adsorption configuration will be discussed below in relation to DFT calculations.

**Kondo Effect in Self-Assembly.** To investigate the arising of a Kondo effect in the commensurate self-assembly, STS and UPS were carried out. Results are displayed in Figure 4. To start with, STS was recorded over a large bias voltage range to investigate the overall electronic properties of the interface. Whereas the UPS probe occupied states only, STS gives access to energy regions above and below the Fermi level in a single-shot experiment enabling a direct comparison with UPS and TPPE spectra of previous studies.<sup>38,39</sup> The differential conductance  $dI/dV$  spectrum in Figure 4a reveals distinct peaks that can unambiguously be assigned. Peaks located at about  $-0.12$  and  $-1.2$  V are attributed to F-LUMO and HOMO, respectively, according to refs 38 and 104. At positive bias, the steplike feature which is typical of a nearly free

electron two-dimensional gas is assigned to the HIS. Its edge is located at  $+0.23 \pm 0.01$  V, in very good agreement with the band edge measured by TPPE.<sup>39</sup> The F-LUMO and HOMO states are also detected by UPS as indicated in Figure S5. As already explained in ref 38, the presence of an occupied F-LUMO state results from the charge transfer from the Ag surface to the molecule. Hence, both our STS and UPS experiments show that the molecule is negatively charged, in agreement with these previous results. As well as for single molecules, a resonance at  $E_F$  was obtained by using STS and UPS techniques. Bringing forward the same arguments as for the case of single molecules, one can conclude that this resonance is the experimental signature of the Kondo effect. A high-resolution STS spectrum in Figure 4b exhibits, as in the case of single 2HPc, an extra peak at about 50 meV, leading to the conclusion that electron–vibron coupling is not hindered by intermolecular interactions inside the self-assembly, thus resulting in a vibrational Kondo effect. Once again, this is corroborated by the inelastic electron tunneling spectrum shown by the blue line in Figure 4b recorded over the Pc ligand and exhibiting the characteristic symmetric two-step-like line shape. The Kondo temperature  $T_K$  obtained by fitting the STS spectra recorded over seven molecules inside the supramolecular network ranges from 57 to 69 K as displayed in Figure S2. It is about twice smaller than for single molecules. Possible explanations for the difference between the two phases will be discussed in the Discussion section.

**Density of States Calculated by DFT.** To correlate spectroscopic peaks observed in STS and UPS spectra with the molecular electronic structure, we have computed the DOS of 2HPc in the C-phase and projected it onto atomic orbitals. As shown in Figure 4d, this PDOS is dominated by  $p_z$  orbitals. One peak below  $-1$  eV corresponds to the HOMO state. Crossing  $E_F$ , another prominent peak of  $p_z$  character corresponds to the F-LUMO state. Although the calculated energy position of this state is upshifted compared to experiments due to a well-known drawback of standard DFT calculations that do not properly account for HOMO–LUMO gap, it remains in good agreement with experimental data and supports the identification of the electronic states of the  $dI/dV$  spectrum of Figure 4a.

A net charge transfer of  $0.32 e^-$  of sp-orbital character occurs from the substrate to the adsorbate region. Again, this value is only qualitative since charge transfer estimated from DFT calculations depends critically on the computational details.<sup>105</sup> Spin density distributions have been calculated as well and are shown in Figure 4e. Obviously, the no-spin-bearing free 2HPc molecule does not exhibit any spin density (Figure 4e, left). However, upon adsorption on Ag(111) (Figure 4e, right), we observe a distribution of the spin electron density in the inner region of the molecule situated mostly on the pyrrole parts. This is very similar to what is observed for the anionic species as displayed in Figure 4e (center panel). The DFT results confirm the scenario that the origin of the Kondo effect lies in the filling of the molecular  $\pi$  states occurring upon adsorption on the silver surface.

**Electronic Surface Properties of Ag(111).** To utterly describe the organometallic interface, the Ag properties must be investigated as well. Moreover, their knowledge will help us better understand the Kondo effect. In the following, we are interested in the modifications of the Ag surface properties when a very small amount of molecules is adsorbed such as in Figure 1b. To begin with, we have recorded a  $dI/dV$  curve on pristine Ag(111) prior to molecular adsorption. It is shown as a gray dashed curve in Figure 5a. Its line shape and energy onset are typical of the well-known Ag Shockley surface state.<sup>68,106,107</sup> After molecular adsorption at low coverage,  $dI/dV$  spectra have been recorded on the uncovered Ag surface in between molecules. They are quite different compared to the one observed on the pristine Ag surface, and they depend strongly on the location where they were recorded. Spectra 2–4 are given in Figure 5a as examples. The spectra can be described as a step-like line shape with prominent peaks superimposed to it. As will be explained below, those extra peaks are eigenstates resulting from electron confinement. STM and conductance maps are shown in Figure 5c–f. A strong spatially textured background between the molecules is observed for energies  $eV_b$  above the Ag Shockley state energy onset  $E_0$ . This is illustrated by the STM image recorded at  $-40$  meV in Figure 5b. The effect is even better evidenced on the three conductance maps shown in Figure 5c–f. Indeed, whereas the  $dI/dV$  map recorded at  $-0.1$  V in (c) shows a constant and homogeneous background, strong variation of the conductance is observed on the flat areas of bare Ag between the molecules for the map at  $eV_b > E_0$  in Figure 5d–f. Moreover, it depends strongly on the energy. Because of these characteristics, we attribute these observations to the formation of standing wave patterns resulting from the scattering of the 2D nearly free electron surface state of Ag. In other words, 2HPc molecules act as electron scatterers of nanometric size.

In those maps, the most surprising feature is the one observed at the center of the image as pointed by the green arrow in Figure 5d–f that is reminiscent of electron confinement in closed 2D artificial hexagonal Ag nanovacancies,<sup>108</sup> nanoislands,<sup>109–111</sup> or even 2D porous molecular networks adsorbed on coinage (111) metal surfaces.<sup>112</sup> What is remarkable is that contrary to those 2D resonators that are closed structures delimited by hard walls, the patterns of this current work have been obtained with only 4 or 5 molecules that are 2–5 nm apart and thus forming an open structure. In the above-mentioned examples of electron confinement, the potential barrier is considered as continuous whereas it is obviously discontinuous in the present work. Shchyrba et al. showed previously partial confinement insides molecular pores with missing borders.<sup>113</sup> Pennec et al. showed confinement of the Ag surface state in a U-shaped cavity formed of linear molecular walls. However, to the best of our knowledge, the formation of an open walls molecular confining cavity has not been evidenced yet and therefore deserves a keen interest.

Scattering of the surface state of (111) surfaces of coinage metals by  $\pi$ -conjugated molecules has been previously observed.<sup>114–118</sup> When self-assembled in specific ways such as in ref 117 or organized in metal–organic frameworks, molecules can act as scattering walls for electrons of a two-dimensional electron gas. Quantum well arrays can thus be formed with well-defined molecular boundaries. A single  $\pi$ -conjugated molecular scatterer has been modeled<sup>114</sup> as a collection of atomic total absorbers at the position of the carbon atoms using multiple scattering expansion as developed for quantum corrals.<sup>119</sup> In molecular porous networks, scattering molecules are described in the framework of the boundary elements method where molecular boundaries correspond to constant rectangular potential.<sup>116</sup> The case of 2HPc on Ag(111) at low coverage is singular in the sense that it represents an intermediate case between the two situations cited above. Therefore, to explain the patterns observed in our work, a complementary theoretical approach might be necessary, and further experimental investigations are required. This demonstrates that the 2HPc/Ag(111) interface offers the possibility to explore new fundamental aspects of quantum physics, i.e., the electron scattering by an object of nanometric size composed of a collection of atomic-like scatterers covalently bonded. Besides, it holds promise for the design of tunable low-dimensional electron resonator. As will be discussed in the Discussion section, quantum confinement might have a nonnegligible impact on the Kondo effect.

## ■ DISCUSSION

In this section, we would like to address the mechanism behind the variation of  $T_K$  within the G-phase as well as with molecular density. In previous sections we have shown that  $T_K$  for single molecules can vary by about several tens of kelvin. In addition, it is about twice smaller in the C-phase as compared with the G-phase.

Prior to that, the question arises whether the UPS spectra of the two phases corroborate STS results. To answer it, a quantitative extraction of  $T_K$  would be necessary. However, such analysis requires a temperature dependence of the line width of the Kondo peak together with theoretical calculations of the spectral function.<sup>120</sup> Solely based on (i) the width and intensity of the Kondo resonance which are larger for the C-phase than for the G-phase, (ii) theoretical descriptions of the variation of the spectral function,<sup>87</sup> and (iii) experimental

photoemission intensity of heavy fermion systems as a function of  $T_K$ ,<sup>87,89,90,120</sup> we would conclude that the C-phase has a higher  $T_K$  than the G-phase. This would contradict our STS measurements. However, in the present case, a direct parallel with those available works on strongly correlated materials is not totally valid since the  $\pi$ -orbital is involved instead of 4f states. In addition, here, electron–vibron coupling related to vibrational energies very close to  $E_F$  is present. The presence of such a coupling might result in satellite Kondo resonances at energies related to  $E_\nu$  and therefore might contribute to the width of the UPS spectra in the close vicinity of  $E_F$ .<sup>98</sup> The intensity of the coupling is likely to vary between the two phases, thus affecting differently the intensity and the width of the corresponding resonances. Further theoretical work is required to properly describe molecular vibrational Kondo effect and to analyze experimental UPS line shape when charge–vibron coupling is present in a Kondo system. As a conclusion, the following discussion can only be based on  $T_K$  extracted from STS.

The Kondo temperature inside the G-phase can be assumed to depend on the adsorption configuration.<sup>53</sup> Nevertheless, it is not supported by our DFT calculations: adsorption heights and PDOS are very similar for both  $\alpha$  and  $\beta$  configurations. Comparing the G- and C-phase, a possible explanation could lie in the effect of intermolecular interactions. It has been shown in some Pc supramolecular assemblies that ligand–ligand interaction could engender a lifting of the molecules, reducing the molecule–substrate coupling and thus  $T_K$ .<sup>28,56</sup> However, according to our DFT calculations, the adsorption height varies only minutely between the two phases. In addition, as shown in Figure S6, the PDOS of the 2HPc molecule on Ag(111) at low concentration is very similar to the one of molecules in the C-phase reported in Figure 4d. The position of the F-LUMO varies only a little, and a charge transfer of 0.27 electrons has been extracted. This is very close to the value of 0.32 electrons obtained for the self-assembly. This supposes that the coupling strength with the substrate does not vary much upon formation of the C-phase and cannot account for the strong variation of  $T_K$ .

The Ruderman–Kittel–Kasuya–Yosida (RKKY) interaction is an alternative origin. It is an indirect spin–spin interaction mediated by the conduction electrons of the metal. Depending on distance, it favors ferromagnetic or antiferromagnetic (AFM) alignments of single magnetic moments. It has been shown that an interplay between the Kondo effect and the RKKY interaction exists in supramolecular assemblies as well.<sup>52,62</sup> The width of the Abrikosov–Suhl resonance is strongly affected or even suppressed due to the magnetic coupling between the spins. More specifically, FM RKKY interaction sharpens the resonance and, on the other hand, the AFM RKKY broadens it.<sup>121</sup> Unfortunately, it is very challenging to test the assumption whether RKKY interaction is responsible for the reduction of  $T_K$  in the self-assembly. Indeed, to demonstrate it, a thought experiment would be to measure  $T_K$  by STS as a function of the molecule–molecule distance for a pair of molecules to mimic the conditions of the two-impurities Kondo problem.<sup>122</sup> However, in such a case of a molecular pair, surface electrons would dominate the RKKY interaction due to their lower  $k_F$  compared to bulk electrons and could not be used to conclude on the exchange coupling in the self-assembly for which the surface state has hybridized with a molecular orbital to form the unoccupied HIS. Nevertheless, one can tentatively apply the following formula

to predict the sign of the exchange coupling in the commensurate phase:  $J = J_0 \frac{\sin(2k_F r)}{(2k_F r)^2}$ , where  $k_F$  is the Fermi wave vector of the substrate and  $r$  is the distance between the spins. The latter parameter  $r$  can be estimated from the calculated lattice parameters of the rectangular unit cell (black dashed line in Figure 2c) that are equal to 1.51 and 1.45 nm and  $k_F = 12.02 \text{ nm}^{-1}$ .<sup>123</sup> Moreover, we discard the influence of the second-nearest neighbors due to the fast decay of the exchange for bulk electrons. The result gives an AFM coupling between nearest-neighbors molecules. This would lead to an increase of  $T_K$  compared with the single impurity case which contradicts our experimental findings. Therefore, RKKY cannot account for the decrease of  $T_K$  upon formation of self-assembly.

The observed variation of  $T_K$  between the two phases could be alternatively explained considering that  $T_K$  is directly proportional to  $\exp(-1/\rho_F)$ , where  $\rho_F$  is the substrate’s density of states at the Fermi energy and  $J$  is the exchange coupling at the magnetic impurity.<sup>87</sup> This relationship indicates that when  $\rho_F$  is reduced,  $T_K$  is reduced as a result. At low molecular concentration, the uncovered substrate exhibits a Shockley surface state that participates to  $\rho_F$ . In the case of the C-phase, as this state hybridizes with the LUMO state of the free molecule to form the HIS shifted above  $E_F$ ,  $\rho_F$  is reduced in comparison with the isolated molecules and thus would explain the decrease of  $T_K$  for the C-phase.

The influence of the surface state on the Kondo resonance width has been a topic of debate for many years (see ref 124 and references therein). Some works on Ag(111) have suggested a minor role for surface-state electrons in the Kondo effect.<sup>125</sup> Only very recently Li et al. tackled this controversy by using LT-STM/STS on Co adsorbates on Ag(111).<sup>124</sup> They unambiguously demonstrated the influence of the surface state on the Kondo resonance by measuring the width of the zero-bias peak as a function of the lateral distance to the impurity. The key point is that they evidenced an oscillatory dependency as a function of the distance to the magnetic impurity which periodicity matches the half Fermi wavelength of the Ag(111) surface state. Moro-Lagares et al. obtained experimentally and theoretically a nearly linear relationship between  $T_K$  and the surface-state contribution to the local density of states of the substrate.<sup>126</sup> Besides, both works emphasize the effect of quantum confinement of the surface state. In particular, it was evidenced that in a quantum corral the Kondo width can be significantly increased (more than 3 times).<sup>124</sup> As at low molecular density in the 2HPc/Ag(111) system, quantum confinement of the Ag surface state is also observed; it probably also plays a significant role in the high value of  $T_K$  and its variation in the G-phase. The effect of the Shockley surface state on  $T_K$  has also been observed on molecules such as Co–tetraphenylporphyrin on Cu(111).<sup>115</sup> In this work, Iancu et al. showed that molecules exposed to Cu surface state electrons exhibit a higher  $T_K$  than molecules inside a self-assembled cluster. These results are in favor of our observation of a lower  $T_K$  upon self-assembly.

## ■ CONCLUSIONS

As a conclusion, we have studied the electronic properties of the metal-free phthalocyanine 2HPc adsorbed on Ag(111) surfaces by means of scanning tunneling and photoelectron spectroscopies and compared the experimental results with DFT calculations. We have evidenced a partial filling of a

molecular  $\pi$  state lying next to the Fermi level. The presence of this extra  $\pi$ -spin in the molecule leads to the emergence of a Kondo effect at low temperature for single molecules as well as for molecules arranged in a 2D self-assembly.

The fact that we deal with a metal-free phthalocyanine offers many future prospects. In other words, the absence of a metal ion at the center of the molecule is the asset of this system. Indeed, it has been shown that this metal-free central cavity of 2HPc can be manipulated by STM in many ways: tautomerization,<sup>84</sup> partial or total dehydrogenation, or direct Ag metalation can be induced.<sup>46</sup> Therefore, one can envisage to investigate the influence of such modifications on the Kondo physics. As an example, a 2HPc molecule can be transformed into an AgPc molecule in the self-assembly<sup>46</sup> and study the effect on  $T_K$ . In that case,  $T_K$  is likely to change through the modification of the local coupling with the substrate via the up- or down-lifting of the molecules or the RKKY interaction between neighboring molecules.

Besides the STM manipulation-based approach, local modification of the electronic and magnetic properties of 2HPc can be obtained by on-surface synthesis such as chemical doping or metalation upon adsorption of alkali or metallic atoms under UHV.<sup>26,85</sup> By use of Li dopants, the charge transfer could be locally modulated, and the molecular spin could be tuned.<sup>26</sup> In another study, Bai et al. showed that 2HPc reacts strongly with Fe atoms to form FePc molecules on Ag(111).<sup>85</sup> This on-surface metalation process was theoretically shown to be energetically favorable for M = Co, Ni, and Mn on 2HPc/Ag(111).<sup>127</sup> It would be particularly interesting to study the Kondo physics in the MPC/2HPc heteromolecular arrays as a function of MPC concentration. Overall, any combination of the above cited manipulation strategies might be used. For these reasons, this system offers an exceptionally rich playground for investigating the molecular Kondo physics.

## ■ ASSOCIATED CONTENT

### SI Supporting Information

The Supporting Information is available free of charge at <https://pubs.acs.org/doi/10.1021/acs.jpcc.9b11141>.

STS spectra of G- and C-phases and Fano fits; calculated band structure of Ag; sequence of STM images showing in-plane molecular rotation. UPS spectra of G- and C-phases; computed density of states projected onto atomic orbitals of 2HPc molecules on Ag(111) assembled in a  $7 \times 7$  arrangement; details on tip conditions for the observation of the Kondo resonance in STS spectra (PDF)

## ■ AUTHOR INFORMATION

### Corresponding Author

M. Sicot – Université de Lorraine, CNRS, IJL, F-54000 Nancy, France; [orcid.org/0000-0002-0558-2113](https://orcid.org/0000-0002-0558-2113); Email: [muriel.sicot@univ-lorraine.fr](mailto:muriel.sicot@univ-lorraine.fr)

### Authors

J. Granet – Université de Lorraine, CNRS, IJL, F-54000 Nancy, France

I. C. Gerber – Université de Toulouse, INSA-CNRS-UPS, LPCNO, 31077 Toulouse, France; [orcid.org/0000-0001-5091-2655](https://orcid.org/0000-0001-5091-2655)

G. Kremer – Université de Lorraine, CNRS, IJL, F-54000 Nancy, France; Département de Physique and Fribourg Center

for Nanomaterials, Université de Fribourg, CH-1700 Fribourg, Switzerland; [orcid.org/0000-0003-1753-3471](https://orcid.org/0000-0003-1753-3471)

T. Pierron – Université de Lorraine, CNRS, IJL, F-54000 Nancy, France

B. Kierren – Université de Lorraine, CNRS, IJL, F-54000 Nancy, France

L. Moreau – Université de Lorraine, CNRS, IJL, F-54000 Nancy, France

Y. Fagot-Revurat – Université de Lorraine, CNRS, IJL, F-54000 Nancy, France

S. Lamare – Univ. Bourgogne Franche-Comté, FEMTO-ST, CNRS, UFC, F-25030 Cedex Besançon, France

F. Chérioux – Univ. Bourgogne Franche-Comté, FEMTO-ST, CNRS, UFC, F-25030 Cedex Besançon, France; [orcid.org/0000-0002-2906-0766](https://orcid.org/0000-0002-2906-0766)

D. Malterre – Université de Lorraine, CNRS, IJL, F-54000 Nancy, France

Complete contact information is available at:

<https://pubs.acs.org/10.1021/acs.jpcc.9b11141>

## Notes

The authors declare no competing financial interest.

## ■ REFERENCES

- (1) Urtizberea, A.; Natividad, E.; Alonso, P. J.; Andrés, M. A.; Gascón, I.; Goldmann, M.; Roubeau, O. A Porphyrin Spin Qubit and Its 2D Framework Nanosheets. *Adv. Funct. Mater.* **2018**, *28*, 1801695–15.
- (2) Gaita-Ariño, A.; Luis, F.; Hill, S.; Coronado, E. Molecular Spins for Quantum Computation. *Nat. Chem.* **2019**, *11*, 301–309.
- (3) Cavallini, M.; Gomez-Segura, J.; Ruiz-Molina, D.; Massi, M.; Albonetti, C.; Rovira, C.; Veciana, J.; Biscarini, F. Magnetic Information Storage on Polymers by Using Patterned Single-Molecule Magnets. *Angew. Chem., Int. Ed.* **2005**, *44*, 888–892.
- (4) Cinchetti, M.; Dediu, V. A.; Hueso, L. E. Activating the Molecular Spinterface. *Nat. Mater.* **2017**, *16*, 507–515.
- (5) Bogani, L.; Wernsdorfer, W. Molecular Spintronics Using Single-Molecule Magnets. *Nat. Mater.* **2008**, *7*, 179–186.
- (6) Mannini, M.; Pineider, F.; Sainctavit, P.; Danieli, C.; Otero, E.; Sciancalepore, C.; Talarico, A. M.; Arrio, M.-A.; Cornia, A.; Gatteschi, D.; et al. Magnetic Memory of a Single-Molecule Quantum Magnet Wired to a Gold Surface. *Nat. Mater.* **2009**, *8*, 194–197.
- (7) Guo, F.-S.; Day, B. M.; Chen, Y.-C.; Tong, M.-L.; Mansikkamäki, A.; Layfield, R. A. A Dysprosium Metallocene Single-Molecule Magnet Functioning at the Axial Limit. *Angew. Chem., Int. Ed.* **2017**, *56*, 11445–11449.
- (8) Zhao, A.; Li, Q.; Chen, L.; Xiang, H.; Wang, W.; Pan, S.; Wang, B.; Xiao, X.; Yang, J.; Hou, J. G.; Zhu, Q. Controlling the Kondo Effect of an Adsorbed Magnetic Ion Through Its Chemical Bonding. *Science* **2005**, *309*, 1542–1544.
- (9) Li, Z.; Li, B.; Yang, J.; Hou, J. G. Single-Molecule Chemistry of Metal Phthalocyanine on Noble Metal Surfaces. *Acc. Chem. Res.* **2010**, *43*, 954–962.
- (10) Niu, T.; Li, A. Exploring Single Molecules by Scanning Probe Microscopy: Porphyrin and Phthalocyanine. *J. Phys. Chem. Lett.* **2013**, *4*, 4095–4102.
- (11) Komeda, T.; Katoh, K.; Yamashita, M. Double-decker phthalocyanine complex: Scanning Tunneling Microscopy Study of Film Formation and Spin Properties. *Prog. Surf. Sci.* **2014**, *89*, 127–160.
- (12) Ishikawa, N.; Sugita, M.; Ishikawa, T.; Koshihara, S.; Kaizu, Y. Lanthanide Double-Decker Complexes Functioning as Magnets at the Single-Molecular Level. *J. Am. Chem. Soc.* **2003**, *125*, 8694–8695.
- (13) Ishikawa, N.; Sugita, M.; Wernsdorfer, W. Quantum Tunneling of Magnetization in Lanthanide Single-Molecule Magnets: Bis-

- (phthalocyaninato)terbium and Bis(phthalocyaninato)dysprosium Anions. *Angew. Chem., Int. Ed.* **2005**, *44*, 2931–2935.
- (14) Urdampilleta, M.; Klyatskaya, S.; Cleuziou, J.-P.; Ruben, M.; Wernsdorfer, W. Supramolecular Spin Valves. *Nat. Mater.* **2011**, *10*, 502–506.
- (15) Gottfried, J. M. Surface Chemistry of Porphyrins and Phthalocyanines. *Surf. Sci. Rep.* **2015**, *70*, 259–379.
- (16) Amsterdam, S. H.; Stanev, T. K.; Zhou, Q.; Lou, A. J. T.; Bergeron, H.; Darancet, P.; Hersam, M. C.; Stern, N. P.; Marks, T. J. Electronic Coupling in Metallophthalocyanine–Transition Metal Dichalcogenide Mixed-Dimensional Heterojunctions. *ACS Nano* **2019**, *13*, 4183–4190.
- (17) Kafle, T. R.; Kattel, B.; Lane, S. D.; Wang, T.; Zhao, H.; Chan, W.-L. Charge Transfer Exciton and Spin Flipping at Organic–Transition-Metal Dichalcogenide Interfaces. *ACS Nano* **2017**, *11*, 10184–10192.
- (18) Padgaonkar, S.; Amsterdam, S. H.; Bergeron, H.; Su, K.; Marks, T. J.; Hersam, M. C.; Weiss, E. A. Molecular Orientation-Dependent Interfacial Charge Transfer in Phthalocyanine/MoS<sub>2</sub>Mixed-Dimensional Heterojunctions. *J. Phys. Chem. C* **2019**, *123*, 13337–13343.
- (19) Suzuki, T.; Kurahashi, M.; Ju, X.; Yamauchi, Y. Spin Polarization of Metal (Mn, Fe, Cu, and Mg) and Metal-Free Phthalocyanines on an Fe(100) Substrate. *J. Phys. Chem. B* **2002**, *106*, 11553–11556.
- (20) Atodiresei, N.; Brede, J.; Lazić, P.; Caciuc, V.; Hoffmann, G.; Wiesendanger, R.; Blügel, S. Design of the Local Spin Polarization at the Organic-Ferromagnetic Interface. *Phys. Rev. Lett.* **2010**, *105*, 066601.
- (21) Djeghloul, F.; Gruber, M.; Urbain, E.; Xenioti, D.; Joly, L.; Boukari, S.; Arabski, J.; Bulou, H.; Scheurer, F.; Bertran, F.; et al. High Spin Polarization at Ferromagnetic Metal–Organic Interfaces: A Generic Property. *J. Phys. Chem. Lett.* **2016**, *7*, 2310–2315.
- (22) Delprat, S.; Galbiati, M.; Tatay, S.; Quinard, B.; Barraud, C.; Petroff, F.; Seneor, P.; Mattana, R. Molecular Spintronics: the Role of Spin-Dependent Hybridization. *J. Phys. D: Appl. Phys.* **2018**, *51*, 473001.
- (23) Caputo, M.; Panighel, M.; Lisi, S.; Khalil, L.; Santo, G. D.; Papalazarou, E.; Hruban, A.; Konczykowski, M.; Krusin-Elbaum, L.; Aliev, Z. S.; et al. Manipulating the Topological Interface by Molecular Adsorbates: Adsorption of Co-Phthalocyanine on Bi<sub>2</sub>Se<sub>3</sub>. *Nano Lett.* **2016**, *16*, 3409–3414.
- (24) Bauer, J.; Pascual, J. I.; Franke, K. J. Microscopic Resolution of the Interplay of Kondo Screening and Superconducting Pairing: Mn-Phthalocyanine Molecules Adsorbed on Superconducting Pb(111). *Phys. Rev. B: Condens. Matter Mater. Phys.* **2013**, *87*, 075125.
- (25) Malavolti, L.; Briganti, M.; Hänze, M.; Serrano, G.; Cimatti, I.; McMurtrie, G.; Otero, E.; Ohresser, P.; Totti, F.; Mannini, M.; et al. Tunable Spin–Superconductor Coupling of Spin 1/2 Vanadyl Phthalocyanine Molecules. *Nano Lett.* **2018**, *18*, 7955–7961.
- (26) Krull, C.; Robles, R.; Mugarza, A.; Gambardella, P. Site- and Orbital-Dependent Charge Donation and Spin Manipulation in Electron-Doped Metal Phthalocyanines. *Nat. Mater.* **2013**, *12*, 337–343.
- (27) Ballav, N.; Wäckerlin, C.; Siewert, D.; Oppeneer, P. M.; Jung, T. A. Emergence of On-Surface Magnetochemistry. *J. Phys. Chem. Lett.* **2013**, *4*, 2303–2311.
- (28) Mugarza, A.; Krull, C.; Robles, R.; Stepanow, S.; Ceballos, G.; Gambardella, P. Spin Coupling and Relaxation Inside Molecule–Metal Contacts. *Nat. Commun.* **2011**, *2*, 490.
- (29) Mugarza, A.; Robles, R.; Krull, C.; Korytár, R.; Lorente, N.; Gambardella, P. Electronic and Magnetic Properties of Molecule–Metal Interfaces: Transition-Metal Phthalocyanines Adsorbed on Ag(100). *Phys. Rev. B: Condens. Matter Mater. Phys.* **2012**, *85*, 155437–13.
- (30) Anderson, P. W. Localized Magnetic States in Metals. *Phys. Rev.* **1961**, *124*, 41–53.
- (31) Kondo, J. Resistance Minimum in Dilute Magnetic Alloys. *Prog. Theor. Phys.* **1964**, *32*, 37–49.
- (32) Li, J.; Schneider, W.-D.; Berndt, R.; Delley, B. Kondo Scattering Observed at a Single Magnetic Impurity. *Phys. Rev. Lett.* **1998**, *80*, 2893–2896.
- (33) Madhavan, V.; Chen, W.; Jamneala, T.; Crommie, M. F.; Wingreen, N. S. Tunneling into a Single Magnetic Atom: Spectroscopic Evidence of the Kondo Resonance. *Science* **1998**, *280*, 567–569.
- (34) Komeda, T. Spins of Adsorbed Molecules Investigated by the Detection of Kondo Resonance. *Surf. Sci.* **2014**, *630*, 343–355.
- (35) Ternes, M.; Heinrich, A. J.; Schneider, W.-D. Spectroscopic Manifestations of the Kondo Effect on Single Adatoms. *J. Phys.: Condens. Matter* **2009**, *21*, 053001.
- (36) Toader, M.; Shukryna, P.; Knupfer, M.; Zahn, D. R. T.; Hietschold, M. Site-Dependent Donation/Backdonation Charge Transfer at the CoPc/Ag(111) Interface. *Langmuir* **2012**, *28*, 13325–13330.
- (37) Gorgoi, M.; Zahn, D. R. Charge-Transfer at Silver/Phthalocyanines Interfaces. *Appl. Surf. Sci.* **2006**, *252*, 5453–5456.
- (38) Kröger, I.; Bayersdorfer, P.; Stadtmüller, B.; Kleimann, C.; Mercurio, G.; Reinert, F.; Kumpf, C. Submonolayer Growth of H<sub>2</sub>-Phthalocyanine on Ag(111). *Phys. Rev. B: Condens. Matter Mater. Phys.* **2012**, *86*, 195412.
- (39) Caplins, B. W.; Suich, D. E.; Shearer, A. J.; Harris, C. B. Metal/Phthalocyanine Hybrid Interface States on Ag(111). *J. Phys. Chem. Lett.* **2014**, *5*, 1679–1684.
- (40) Fernández-Torrente, I.; Franke, K. J.; Pascual, J. I. Vibrational Kondo Effect in Pure Organic Charge-Transfer Assemblies. *Phys. Rev. Lett.* **2008**, *101*, 217203.
- (41) Choi, T.; Bedwani, S.; Rochefort, A.; Chen, C.-Y.; Epstein, A. J.; Gupta, J. A. A Single Molecule Kondo Switch: Multistability of Tetracyanoethylene on Cu(111). *Nano Lett.* **2010**, *10*, 4175–4180.
- (42) Liu, J.; Isshiki, H.; Katoh, K.; Morita, T.; Breedlove, B. K.; Yamashita, M.; Komeda, T. First Observation of a Kondo Resonance for a Stable Neutral Pure Organic Radical, 1,3,5-Triphenyl-6-oxoverdazyl, Adsorbed on the Au(111) Surface. *J. Am. Chem. Soc.* **2013**, *135*, 651–658.
- (43) Requist, R.; Modesti, S.; Baruselli, P. P.; Smogunov, A.; Fabrizio, M.; Tosatti, E. Kondo Conductance Across the Smallest Spin 1/2 Radical Molecule. *Proc. Natl. Acad. Sci. U. S. A.* **2014**, *111*, 69–74.
- (44) Esat, T.; Lechtenberg, B.; Deilmann, T.; Wagner, C.; Krüger, P.; Temirov, R.; Rohlfing, M.; Anders, F. B.; Tautz, F. S. A Chemically Driven Quantum Phase Transition in a Two-Molecule Kondo System. *Nat. Phys.* **2016**, *12*, 867–873.
- (45) Karan, S.; Li, N.; Zhang, Y.; He, Y.; Hong, I.-P.; Song, H.; Lü, J.-T.; Wang, Y.; Peng, L.; Wu, K.; et al. Spin Manipulation by Creation of Single-Molecule Radical Cations. *Phys. Rev. Lett.* **2016**, *116*, 027201.
- (46) Sperl, A.; Kröger, J.; Berndt, R. Controlled Metalation of a Single Adsorbed Phthalocyanine. *Angew. Chem., Int. Ed.* **2011**, *50*, 5294–5297.
- (47) Perera, U. G. E.; Kulik, H. J.; Iancu, V.; da Silva, L. G. G. V. D.; Ulloa, S. E.; Marzari, N.; Hla, S.-W. Spatially Extended Kondo State in Magnetic Molecules Induced by Interfacial Charge Transfer. *Phys. Rev. Lett.* **2010**, *105*, 106601.
- (48) Booth, C. H.; Walter, M. D.; Daniel, M.; Lukens, W. W.; Andersen, R. A. Self-Contained Kondo Effect in Single Molecules. *Phys. Rev. Lett.* **2005**, *95*, 267202.
- (49) Wahl, P.; Diekhöner, L.; Wittich, G.; Vitali, L.; Schneider, M. A.; Kern, K. Kondo Effect of Molecular Complexes at Surfaces: Ligand Control of the Local Spin Coupling. *Phys. Rev. Lett.* **2005**, *95*, 166601.
- (50) Zhao, A.; Hu, Z.; Wang, B.; Xiao, X.; Yang, J.; Hou, J. G. Kondo Effect in Single Cobalt Phthalocyanine Molecules Adsorbed on Au(111) Monoatomic Steps. *J. Chem. Phys.* **2008**, *128*, 234705.
- (51) Scott, G. D.; Natelson, D. Kondo Resonances in Molecular Devices. *ACS Nano* **2010**, *4*, 3560–3579.

- (52) Tsukahara, N.; Shiraki, S.; Itou, S.; Ohta, N.; Takagi, N.; Kawai, M. Evolution of Kondo Resonance from a Single Impurity Molecule to the Two-Dimensional Lattice. *Phys. Rev. Lett.* **2011**, *106*, 187201.
- (53) Minamitani, E.; Tsukahara, N.; Matsunaka, D.; Kim, Y.; Takagi, N.; Kawai, M. Symmetry-Driven Novel Kondo Effect in a Molecule. *Phys. Rev. Lett.* **2012**, *109*, 086602.
- (54) Ziroff, J.; Hame, S.; Kochler, M.; Bendounan, A.; Schöll, A.; Reinert, F. Low-Energy Scale Excitations in the Spectral Function of Organic Monolayer Systems. *Phys. Rev. B: Condens. Matter Mater. Phys.* **2012**, *85*, 161404.
- (55) Garnica, M.; Stradi, D.; Barja, S.; Calleja, F.; Diaz, C.; Alcami, M.; Martin, N.; Vázquez de Parga, A. L.; Martin, F.; Miranda, R. Long-Range Magnetic Order in a Purely Organic 2D Layer Adsorbed on Epitaxial Graphene. *Nat. Phys.* **2013**, *9*, 368–374.
- (56) Komeda, T.; Isshiki, H.; Liu, J.; Katoh, K.; Shirakata, M.; Breedlove, B. K.; Yamashita, M. Variation of Kondo Peak Observed in the Assembly of Heteroleptic 2,3-Naphthalocyaninato Phthalocyaninato Tb(III) Double-Decker Complex on Au(111). *ACS Nano* **2013**, *7*, 1092–1099.
- (57) Iancu, V.; Braun, K.-F.; Schouteden, K.; Van Haesendonck, C. Inducing Magnetism in Pure Organic Molecules by Single Magnetic Atom Doping. *Phys. Rev. Lett.* **2014**, *113*, 106102.
- (58) Lin, T.; Kuang, G.; Wang, W.; Lin, N. Two-Dimensional Lattice of Out-of-Plane Dinuclear Iron Centers Exhibiting Kondo Resonance. *ACS Nano* **2014**, *8*, 8310–8316.
- (59) Zhang, Q.; Kuang, G.; Pang, R.; Shi, X.; Lin, N. Switching Molecular Kondo Effect via Supramolecular Interaction. *ACS Nano* **2015**, *9*, 12521–12528.
- (60) Maughan, B.; Zahl, P.; Sutter, P.; Monti, O. L. A. Ensemble Control of Kondo Screening in Molecular Adsorbates. *J. Phys. Chem. Lett.* **2017**, *8*, 1837–1844.
- (61) Hiraoka, R.; Minamitani, E.; Arafune, R.; Tsukahara, N.; Watanabe, S.; Kawai, M.; Takagi, N. Single-molecule quantum dot as a Kondo simulator. *Nat. Commun.* **2017**, *8*, 1–7.
- (62) Tuerhong, R.; Ngassam, F.; Watanabe, S.; Onoe, J.; Alouani, M.; Bucher, J.-P. Two-Dimensional Organometallic Kondo Lattice with Long-Range Antiferromagnetic Order. *J. Phys. Chem. C* **2018**, *122*, 20046–20054.
- (63) Temirov, R.; Soubatch, S.; Luican, A.; Tautz, F. S. Free-Electron-Like Dispersion in an Organic Monolayer Film on a Metal Substrate. *Nature* **2006**, *444*, 350–353.
- (64) Armbrust, N.; Schiller, F.; Güdde, J.; Höfer, U. Model Potential for the Description of Metal/Organic Interface States. *Sci. Rep.* **2017**, *7*, 1–8.
- (65) Lerch, A.; Fernandez, L.; Ilyn, M.; Gastaldo, M.; Paradinas, M.; Valbuena, M. A.; Mugarza, A.; Ibrahim, A. B. M.; Sundermeyer, J.; Höfer, U.; et al. Electronic Structure of Titanylphthalocyanine Layers on Ag(111). *J. Phys. Chem. C* **2017**, *121*, 25353–25363.
- (66) Gerbert, D.; Hofmann, O. T.; Tegeeder, P. Formation of Occupied and Unoccupied Hybrid Bands at Interfaces between Metals and Organic Donors/Acceptors. *J. Phys. Chem. C* **2018**, *122*, 27554–27560.
- (67) Sabitova, A.; Temirov, R.; Tautz, F. S. Lateral Scattering Potential of the PTCDA/Ag(111) Interface State. *Phys. Rev. B: Condens. Matter Mater. Phys.* **2018**, *98*, 205429.
- (68) Bürgi, L.; Knorr, N.; Brune, H.; Schneider, M.; Kern, K. Two-Dimensional Electron Gas at Noble-Metal Surfaces. *Appl. Phys. A: Mater. Sci. Process.* **2002**, *75*, 141–145.
- (69) Reinert, F.; Nicolay, G.; Schmidt, S.; Ehm, D.; Hüfner, S. Direct Measurements of the L-gap Surface States on the (111) Face of Noble Metals by Photoelectron Spectroscopy. *Phys. Rev. B: Condens. Matter Mater. Phys.* **2001**, *63*, 115415.
- (70) Puschnig, P.; Berkebile, S.; Fleming, A. J.; Koller, G.; Emtsev, K.; Seyller, T.; Riley, J. D.; Ambrosch-Draxl, C.; Netzer, F. P.; Ramsey, M. G. Reconstruction of Molecular Orbital Densities from Photoemission Data. *Science* **2009**, *326*, 702–706.
- (71) Gargiani, P.; Betti, M. G.; Taleb-Ibrahimi, A.; Le Fèvre, P.; Modesti, S. Orbital Symmetry of the Kondo State in Adsorbed FePc Molecules on the Au(110) Metal Surface. *J. Phys. Chem. C* **2016**, *120*, 28527–28532.
- (72) Kresse, G.; Hafner, J. *Phys. Rev. B: Condens. Matter Mater. Phys.* **1993**, *47*, 558–561.
- (73) Kresse, G.; Hafner, J. Ab Initio Molecular Dynamics for Liquid Metals. *Phys. Rev. B: Condens. Matter Mater. Phys.* **1994**, *49*, 14251–14269.
- (74) Kresse, G.; Furthmüller, J. Efficient Iterative Schemes for Ab Initio Total-Energy Calculations Using a Plane-Wave Basis Set. *Phys. Rev. B: Condens. Matter Mater. Phys.* **1996**, *54*, 11169–11186.
- (75) Kresse, G.; Furthmüller, J. Efficiency of Ab-Initio Total Energy Calculations for Metals and sSemiconductors Using a Plane-Wave Basis Set. *Comput. Mater. Sci.* **1996**, *6*, 15–50.
- (76) Blöchl, P. E. Projector Augmented-Wave Method. *Phys. Rev. B: Condens. Matter Mater. Phys.* **1994**, *50*, 17953–17979.
- (77) Kresse, G.; Joubert, D. From Ultrasoft Pseudopotentials to the Projector Augmented-Wave Method. *Phys. Rev. B: Condens. Matter Mater. Phys.* **1999**, *59*, 1758–1775.
- (78) Perdew, J. P.; Burke, K.; Ernzerhof, M. Generalized Gradient Approximation Made Simple. *Phys. Rev. Lett.* **1996**, *77*, 3865–3868.
- (79) Grimme, S.; Antony, J.; Ehrlich, S.; Krieg, H. A Consistent and Accurate Ab Initio Parametrization of Density Functional Dispersion Correction (DFT-D) for the 94 elements H-Pu. *J. Chem. Phys.* **2010**, *132*, 154104.
- (80) Bučko, T.; Hafner, J.; Lebègue, S.; Ángyán, J. G. Improved Description of the Structure of Molecular and Layered Crystals: Ab Initio DFT Calculations with van der Waals Corrections. *J. Phys. Chem. A* **2010**, *114*, 11814–11824.
- (81) Huang, Y.; Wruss, E.; Egger, D.; Kera, S.; Ueno, N.; Saidi, W.; Bucko, T.; Wee, A.; Zojer, E. Understanding the Adsorption of CuPc and ZnPc on Noble Metal Surfaces by Combining Quantum-Mechanical Modelling and Photoelectron Spectroscopy. *Molecules* **2014**, *19*, 2969–2992.
- (82) Blöchl, P. E.; Jepsen, O.; Andersen, O. K. Improved Tetrahedron Method for Brillouin-Zone Integrations. *Phys. Rev. B: Condens. Matter Mater. Phys.* **1994**, *49*, 16223–16233.
- (83) Zaitsev, N. L.; Nechaev, I. A.; Echenique, P. M.; Chulkov, E. V. Transformation of the Ag(111) Surface State Due to Molecule-Surface Interaction with Ordered Organic Molecular Monolayers. *Phys. Rev. B: Condens. Matter Mater. Phys.* **2012**, *85*, 115301.
- (84) Kügel, J.; Sixta, A.; Böhme, M.; Krönlein, A.; Bode, M. Breaking Degeneracy of Tautomerization—Metastability from Days to Seconds. *ACS Nano* **2016**, *10*, 11058–11065.
- (85) Bai, Y.; Buchner, F.; Wendahl, M. T.; Kellner, I.; Bayer, A.; Steinrück, H.-P.; Marbach, H.; Gottfried, J. M. Direct Metalation of a Phthalocyanine Monolayer on Ag(111) with Coadsorbed Iron Atoms. *J. Phys. Chem. C* **2008**, *112*, 6087–6092.
- (86) Nilson, K.; Åhlund, J.; Shariati, M. N.; Schiessling, J.; Palmgren, P.; Brena, B.; Göthelid, E.; Hennies, F.; Huismans, Y.; Evangelista, F.; et al. Potassium-Intercalated H<sub>2</sub>Pc films: Alkali-Induced Electronic and Geometrical Modifications. *J. Chem. Phys.* **2012**, *137*, 044708.
- (87) Hewson, A. C. *The Kondo Problem to Heavy Fermions*; Cambridge University Press: Cambridge, UK, 1993.
- (88) Nagaoka, K.; Jamneala, T.; Grobis, M.; Crommie, M. F. Temperature Dependence of a Single Kondo Impurity. *Phys. Rev. Lett.* **2002**, *88*, 1497.
- (89) Gunnarsson, O.; Schönhammer, K. Electron Spectroscopies for Ce Compounds in the Impurity Model. *Phys. Rev. B: Condens. Matter Mater. Phys.* **1983**, *28*, 4315–4341.
- (90) Malterre, D.; Grioni, M.; Baer, Y. Recent Developments in High-Energy Spectroscopies of Kondo Systems. *Adv. Phys.* **1996**, *45*, 299–348.
- (91) Bickers, N. E.; Cox, D. L.; Wilkins, J. W. Self-Consistent Large-N Expansion for Normal-State Properties of Dilute Magnetic Alloys. *Phys. Rev. B: Condens. Matter Mater. Phys.* **1987**, *36*, 2036–2079.
- (92) Patthey, F.; Imer, J.-M.; Schneider, W.-D.; Beck, H.; Baer, Y.; Delley, B. High-Resolution Photoemission Study of the Low-Energy Excitations in 4f-Electron Systems. *Phys. Rev. B: Condens. Matter Mater. Phys.* **1990**, *42*, 8864–8881.

- (93) Costi, T. A. Kondo Effect in a Magnetic Field and the Magnetoresistivity of Kondo Alloys. *Phys. Rev. Lett.* **2000**, *85*, 1504–1507.
- (94) König, J.; Schoeller, H.; Schön, G. Zero-Bias Anomalies and Boson-Assisted Tunneling Through Quantum Dots. *Phys. Rev. Lett.* **1996**, *76*, 1715–1718.
- (95) Flensberg, K. Tunneling Broadening of Vibrational Sidebands in Molecular Transistors. *Phys. Rev. B: Condens. Matter Mater. Phys.* **2003**, *68*, 205323.
- (96) Paaske, J.; Flensberg, K. Vibrational Sidebands and the Kondo Effect in Molecular Transistors. *Phys. Rev. Lett.* **2005**, *94*, 176801.
- (97) Chen, Z.-Z.; Lu, H.; Lu, R.; Zhu, B.-f. Phonon-Assisted Kondo Effect in a Single-Molecule Transistor out of Equilibrium. *J. Phys.: Condens. Matter* **2006**, *18*, 5435–5446.
- (98) Roura-Bas, P.; Tosi, L.; Aligia, A. A. Nonequilibrium Transport Through Magnetic Vibrating Molecules. *Phys. Rev. B: Condens. Matter Mater. Phys.* **2013**, *87*, 195136.
- (99) Parks, J. J.; Champagne, A. R.; Hutchison, G. R.; Flores-Torres, S.; Abruña, H. D.; Ralph, D. C. Tuning the Kondo Effect with a Mechanically Controllable Break Junction. *Phys. Rev. Lett.* **2007**, *99*, 026601.
- (100) Iancu, V.; Schouteden, K.; Li, Z.; Van Haesendonck, C. Electron-Phonon Coupling in Engineered Magnetic Molecules. *Chem. Commun.* **2016**, *52*, 11359–11362.
- (101) Endlich, M.; Gozdzik, S.; Néel, N.; da Rosa, A. L.; Frauenheim, T.; Wehling, T. O.; Kröger, J. Phthalocyanine Adsorption to Graphene on Ir (111): Evidence for Decoupling from Vibrational Spectroscopy. *J. Chem. Phys.* **2014**, *141*, 184308.
- (102) Fano, U. Effects of Configuration Interaction on Intensities and Phase Shifts. *Phys. Rev.* **1961**, *124*, 1866–1878.
- (103) Gruber, M.; Weismann, A.; Berndt, R. The Kondo Resonance Line Shape in Scanning Tunneling Spectroscopy: Instrumental Aspects. *J. Phys.: Condens. Matter* **2018**, *30*, 424001.
- (104) Bidermane, I.; Brumboiu, I. E.; Totani, R.; Grazioli, C.; Shariati-Nilsson, M. N.; Herper, H. C.; Eriksson, O.; Sanyal, B.; Ressel, B.; de Simone, M.; et al. Atomic Contributions to the Valence Band Photoelectron Spectra of Metal-Free, Iron and Manganese Phthalocyanines. *J. Electron Spectrosc. Relat. Phenom.* **2015**, *205*, 92–97.
- (105) Gerber, I. C.; Poteau, R. Critical Assessment of Charge Transfer Estimates in Non-Covalent Graphene Doping. *Theor. Chem. Acc.* **2018**, *137*, 156.
- (106) Li, J.; Schneider, W.-D.; Berndt, R. Local Density of States from Spectroscopic Scanning-Tunneling-Microscope Images: Ag(111). *Phys. Rev. B: Condens. Matter Mater. Phys.* **1997**, *56*, 7656–7659.
- (107) Jeandupeux, O.; Bürgi, L.; Hirstein, A.; Brune, H.; Kern, K. Thermal Damping of Quantum Interference Patterns of Surface-State Electrons. *Phys. Rev. B: Condens. Matter Mater. Phys.* **1999**, *59*, 15926–15934.
- (108) Jensen, H.; Kröger, J.; Berndt, R.; Crampin, S. Electron Dynamics in Vacancy Islands: Scanning Tunneling Spectroscopy on Ag(111). *Phys. Rev. B: Condens. Matter Mater. Phys.* **2005**, *71*, 155417.
- (109) Avouris, P.; Lyo, I.-W. Observation of Quantum-Size Effects at Room Temperature on Metal Surfaces With STM. *Science* **1994**, *264*, 942–945.
- (110) Li, J.; Schneider, W.-D.; Berndt, R.; Crampin, S. Electron Confinement to Nanoscale Ag Islands on Ag(111): A Quantitative Study. *Phys. Rev. Lett.* **1998**, *80*, 3332–3335.
- (111) Tournier-Colletta, C.; Kierren, B.; Fagot-Revurat, Y.; Malterre, D. Phonon Contribution to the Lifetime of Surface State Quasiparticles Confined in Nanopyramids. *Phys. Rev. Lett.* **2010**, *104*, 016802.
- (112) Müller, K.; Enache, M.; Stöhr, M. Confinement properties of 2D porous molecular networks on metal surfaces. *J. Phys.: Condens. Matter* **2016**, *28*, 153003.
- (113) Shchyrba, A.; Martens, S. C.; Wäckerlin, C.; Matena, M.; Ivas, T.; Wadehoff, H.; Stöhr, M.; Jung, T. A.; Gade, L. H. Covalent Assembly of a Two-Dimensional Molecular “Sponge” on a Cu(111) Surface: Confined Electronic Surface States in Open and Closed Pores. *Chem. Commun.* **2014**, *50*, 7628–7631.
- (114) Gross, L.; Moresco, F.; Savio, L.; Gourdon, A.; Joachim, C.; Rieder, K.-H. Scattering of Surface State Electrons at Large Organic Molecules. *Phys. Rev. Lett.* **2004**, *93*, 2797.
- (115) Iancu, V.; Deshpande, A.; Hla, S.-W. Manipulation of the Kondo Effect via Two-Dimensional Molecular Assembly. *Phys. Rev. Lett.* **2006**, *97*, 266603.
- (116) Klappenberger, F.; Kühne, D.; Krenner, W.; Silanes, I.; Arnau, A.; de Abajo, F. J. G.; Klyatskaya, S.; Ruben, M.; Barth, J. V. Tunable Quantum Dot Arrays Formed from Self-Assembled Metal-Organic Networks. *Phys. Rev. Lett.* **2011**, *106*, 026802.
- (117) Seufert, K.; Auwärter, W.; de Abajo, F. J. G.; Ecija, D.; Vijayaraghavan, S.; Joshi, S.; Barth, J. V. Controlled Interaction of Surface Quantum-Well Electronic States. *Nano Lett.* **2013**, *13*, 6130–6135.
- (118) Nicoara, N.; Méndez, J.; Gómez-Rodríguez, J. M. Visualizing the Interface State of PTCDA on Au(111) by Scanning Tunneling Microscopy. *Nanotechnology* **2016**, *27*, 475707.
- (119) Heller, E. J.; Crommie, M. F.; Lutz, C. P.; Eigler, D. M. Scattering and Absorption of Surface Electron Waves in Quantum Corals. *Nature* **1994**, *369*, 464–466.
- (120) Ehm, D.; Hüfner, S.; Reinert, F.; Kroha, J.; Wölfle, P.; Stockert, O.; Geibel, C.; Löhneysen, H. v. High-Resolution Photoemission Study on Low- $T_K$  Ce Systems: Kondo Resonance, Crystal Field Structures, and their Temperature Dependence. *Phys. Rev. B: Condens. Matter Mater. Phys.* **2007**, *76*, 045117.
- (121) Minamitani, E.; Nakanishi, H.; Diño, W. A.; Kasai, H. Spectroscopic Profiles of a Magnetic Dimer on a Metal Surface. *Solid State Commun.* **2009**, *149*, 1241–1243.
- (122) Jayaprakash, C.; Krishna-murthy, H. R.; Wilkins, J. W. Two-Impurity Kondo Problem. *Phys. Rev. Lett.* **1981**, *47*, 737–740.
- (123) Ashcroft, N. W.; Mermin, N. D. *Solid State Physics*; Saunders College: Philadelphia, 1976.
- (124) Li, Q. L.; Zheng, C.; Wang, R.; Miao, B. F.; Cao, R. X.; Sun, L.; Wu, D.; Wu, Y. Z.; Li, S. C.; Wang, B. G.; et al. Role of the Surface State in the Kondo Resonance Width of a Co single Adatom on Ag(111). *Phys. Rev. B: Condens. Matter Mater. Phys.* **2018**, *97*, 035417.
- (125) Limot, L.; Berndt, R. Kondo Effect and Surface-State Electrons. *Appl. Surf. Sci.* **2004**, *237*, 572–576.
- (126) Moro-Lagares, M.; Fernández, J.; Roura-Bas, P.; Ibarra, M. R.; Aligia, A. A.; Serrate, D. Quantifying the Leading Role of the Surface State in the Kondo Effect of Co/Ag(111). *Phys. Rev. B: Condens. Matter Mater. Phys.* **2018**, *97*, 235442.
- (127) Bao, D.-L.; Zhang, Y.-Y.; Du, S.; Pantelides, S. T.; Gao, H.-J. Barrierless On-Surface Metal Incorporation in Phthalocyanine-Based Molecules. *J. Phys. Chem. C* **2018**, *122*, 6678–6683.